

MINIATURE AGE-DATING /MATERIALS-CHARACTERIZATION INSTRUMENT FOR MARS EXPLORATION

Final Report

JPL Task 1017

Soon Sam Kim Thermal and Propulsion Engineering Systems Section (353)
Stephen W.S. McKeever and Michael W. Blair
Department of Physics, Oklahoma State University

A. OBJECTIVES

The objective is to develop a miniature age-dating/material-characterization instrument that will combine the most powerful dosimetric dating techniques, namely thermoluminescence (TL), optically stimulated luminescence (OSL) and electron-spin resonance (ESR).

B. PROGRESS AND RESULTS

1. OSL Optical System Design

OSL Stimulation Source: We have concluded that ultra-bright Nichia GaN diodes offer the best solution for the OSL stimulation. They are available in the three main stimulation ranges for OSL (red, green and blue) with variable powers up to 5W.

Photodetectors: We have evaluated 3 potential photodetectors for OSL based on wavelength range, quantum efficiency and operational temperature. They are Hamamatsu Si Avalanche Photodiode (APD) S5343, Hamamatsu H6240 side-window photomultiplier tube (PMT), and Electron tubes Photodetector module DM0016C.

It seems that the APD module in DC detection mode is not sensitive compared to PMT units produced by Hamamatsu and Electron Tubes Inc. Alternatively, the APD can be operated in photon-counting mode, with appropriate modules. The intrinsic thermal noise of the detectors requires cooling, and this is one of the main drawbacks of the APDs. The PMT module produced by Hamamatsu (H6240) has a higher sensitivity than the one produced by Electron tubes. The slopes of the response curves (at 470 nm) were determined to be 152×10^9 and 98×10^9 counts/W respectively. According to data presented above, it seems that Hamamatsu H6240C is the most sensitive detector.

Calibration Radiation Source: To avoid the use of radioisotopes, we have tested an X-ray system, and identified the Moxtek "Bullet" miniature X-ray source (4W, 40 kVp) as a suitable one. The tube is a transmission anode type, operating at 35 kV and 100 μ A. The tube has a beryllium window that is 0.25 mm thick and 2 mm in diameter. The dose rate delivered to quartz grains at the sample position was determined to be 230 ± 10 mGy/s by calibration against a $^{90}\text{Sr}/^{90}\text{Y}$ beta source of known dose rate.

2. OSL and TL under Martian Temperatures

The low-temperature OSL system: As shown in Fig. 1, the system consists of a cryostat, an irradiation/stimulation unit, and a detection unit. The cryostat is able to cool the sample down to -150°C using liquid nitrogen flow, or to heat up to 200°C using two 50 W pencil heaters (Watlow). The irradiation/stimulation unit is fitted with an X-ray on one side, and a quartz window for optical stimulation on the other side. All can be under vacuum during the experiments. The detection is accomplished by a photomultiplier tube (PMT) operating in photon-counting mode (Standford Research SR400 photon counter). A filter pack containing UV transmitting filters (Hoya U-340, transmission between 290 nm and 390 nm) was used to prevent the stimulation light from reaching the PMT. *Optical stimulation* was with a 100 mW Diode Pump Solid State (DPSS) green laser (532 nm, Extreme Lasers Inc.) operating in continuous-wave mode. An optical fiber bundle was used to direct the laser light through the tunnel and diffuse the light over the sample (Fig. 1). The power of the diffused laser light at the sample position was approximately 10 mW/cm^2 . An electronic shutter was used to control the stimulation. Reproducibility was tested by applying a sequence of bleaching for 600s, irradiation with 5 Gy. The OSL curves practically overlapped, the total OSL intensity varying within 5%.

Low temperature OSL: Preliminary investigations showed an increase in the OSL for measurement at very low temperatures. A possible mechanism for the increase is the effect of temperature on luminescence efficiency. In many materials, the luminescence efficiency of recombination centers is observed to decrease with increasing temperatures. This phenomenon is called thermal quenching and is related to an increase in the probability of non-radiative relaxation with increasing temperature. For the quartz used in this investigation, the luminescence efficiency was studied by monitoring the radioluminescence under constant irradiation as the sample was cooled from room temperature down to -125°C . A monotonic increase in the radioluminescence is observed as the temperature of the sample is lowered (Fig. 2). Thermal quenching of the luminescence centers remains one possible explanation for this phenomenon, although at this point no further investigations were carried out to verify this hypothesis.

Low temperature TL: To understand the effect of the OSL measurement temperature and irradiation temperature in the final OSL output, it is important to characterize the thermal stability and optical sensitivity of trapping states. This can be accomplished by a study of the TL curve at low temperatures. For this study, the quartz samples were irradiated at -125°C with 100 Gy and heated to room temperature at a rate of 0.6°C/s . As seen in Fig. 3, TL emission is observed from -100°C up to room temperature, with a clear peak around -50°C . Although it is difficult to determine the number of components of this TL curve, this low temperature peak indicates the presence of trapping states that are relatively stable at temperatures below -50°C and unstable at higher temperatures. To check for the optical sensitivity of these trapping centers, the same procedure was repeated, introducing a bleaching for 300s at -125°C after irradiation. Comparing the TL curve after bleaching (Fig. 3) with the original TL curve, it can be seen that these trapping levels are optically sensitive. Charges captured at these trapping levels probably contribute to the OSL signal at low temperatures.

Effect of measurement and irradiation temperature: The effect of measurement temperature on the OSL was investigated by irradiating quartz samples at room temperature with 5 Gy and performing the OSL readout at different temperatures, from room temperature down to -100°C . The OSL curves obtained are plotted in Fig. 4. The inset shows the total OSL (area under the curve) as a function of temperature. It can be observed that as the OSL measurement temperature is lowered, the OSL initially decreases, reaching a minimum at -50°C , and then increases again. This behavior can be explained by the combination of two processes: (a) retrapping at the low-temperature trapping states and (b) temperature dependence of the luminescence efficiency. Since the irradiation is performed at room temperature, the same traps are filled every time. However, as the temperature is lowered, trapping states that were thermally unstable start to be stable, which means that they become a competitor for the recombination process. As a result, the OSL signal decreases. However, as the temperature is lowered even more for the OSL measurements, the luminescence efficiency starts to increase, resulting in an increased OSL output. Combination of these two processes explains the data presented in the inset of Fig. 4.

We have also investigated the effect of temperature on the OSL curves when both the irradiation and the OSL measurement are done at the same temperature. For this, the samples were cooled to the specified temperature and bleached for 600s. This was followed by irradiation with 5 Gy and the OSL measurement, still keeping the sample at the same temperature. The result of this investigation is presented in Figure 5. It can be observed that as the temperature is lowered, the OSL output increases significantly (inset of Fig. 5). Again, this can be understood by the presence of optically sensitive trapping levels that are stable at low temperatures, and by the temperature-dependent luminescence efficiency. The lower the sample temperature, the higher the number of stable trapping states which are able to capture the free charge carriers created by the irradiation, and the higher the OSL output will be if the stimulation is performed at the same temperature. Coupled with that, the luminescence efficiency increases at low temperatures, also resulting in an increased OSL output. At this point, these two effects cannot be separated. Both contribute to an increase in the OSL output with decreasing temperatures.

Conclusions for in situ dating on Mars: The results presented above provided some understanding of the temperature effects for irradiation and OSL measurements during in situ dating of Martian sediments. Firstly, all OSL measurements should be performed at the same temperature to avoid variations in the luminescence output caused by variations in the luminescence efficiency and by the competition processes introduced by traps whose stability change in the course of the daily temperature variation. By performing the measurements at the lowest possible temperature, the sensitivity can be increased due to the increased luminescence efficiency. However, trapping states stable at these low temperatures may significantly reduce the signal by capturing the charges that are optically stimulated. By reading the OSL at high temperatures, the competition processes are lessened, but the luminescence efficiency is reduced. At this point, investigation of other materials is necessary to determine the appropriate temperature for OSL stimulation.

The presence of optically active trapping states which are stable at low temperatures highlights the importance of either irradiating the samples at high temperature, or applying a pre-heat to empty these trapping states. Otherwise, the OSL signal will be higher than the natural signal for the same dose, resulting in age underestimation. Although only quartz samples were studied in this first experiments, similar effects are to be expected in other minerals, such as feldspars.

3. Characterization of Luminescence from Martian Simulants

To date, we have tested samples from four Martian SNC meteorites, soil simulant JSC Mars-1, another Martian soil simulant (jeweler's rouge) and various feldspars. We have examined their basic TL and OSL properties. We have investigated the main TL peaks, the OSL dose response curves to determine the maximum estimable radiation doses, and the ability to recover a given laboratory radiation dose (using dosimetric techniques). We have developed procedures for TL and OSL, and obtained the following results.

Most luminescence materials encountered on Mars will probably be of feldspathic origin. For terrestrial TL and OSL dating, currently no accepted single-aliquot methods exist for feldspar dating. So far, attempts to develop such a method have been unsuccessful (Wallinga et. al., 2000). Also, many feldspars suffer from anomalous fading whereby thermally stable signals fade with time (Wintle, 1977). Although many suggestions have been made to either correct or eliminate this phenomenon (Huntley and Lamothe, 2001; Lamothe and Auclair, 1999; Vicossekas, 2000), no accepted method has been developed.

Single Aliquot Regenerative (SAR) Method: To address this issue, we have started to develop a single-aliquot procedure for feldspars that also eliminates anomalous fading. Once a procedure has been developed, further work will be carried out to extend the method to polymineral samples (consisting of quartz, feldspars, and other materials), such that it can be utilized for Mars OSL dating. The eventual goal is to use the procedure to obtain depositional ages for polymineral terrestrial samples with independent age controls.

One basic requirement for a single-aliquot technique is that repeated cycles with a fixed regeneration dose (including preheating and sensitivity-correction procedures) yield the same OSL or TL result (either the same luminescence signal or sensitivity-corrected ratio as in SAR). Five types of feldspars (microcline, anorthoclase, oligoclase, albite, and andesine) have been tested for this requirement in several different ways. The experiments showed that OSL sensitivity changes in feldspars can be corrected using the SAR procedure, but the cutheat (preheat with no holding time) must be equal to the (regeneration) preheat in both temperature and duration. Also, it was found that the sensitivity-correction procedure was largely independent of the relative size of the test dose (as compared to the regeneration dose).

4. ESR Characterization of Martian Simulants

ESR characterization of the previously discussed feldspars (microcline, anorthoclase, oligoclase, albite, and andesine) has been undertaken at JPL. The ESR signals from these feldspars are less sensitive to radiation than OSL, since an increase in ESR signal was not seen until the samples had been exposed to 250-500 Gy of irradiation. Also, the OSL and ESR signals do not appear to arise from the same traps, as bleaching had little effect on the ESR signals.

We have constructed an ESR dose-response curve for oligoclase, using an additive-dose procedure without preheating. The sample was subjected to repeated cycles of irradiation and ESR measurement (which does not erase the stored dose), so that the dose is the total accumulated dose. Even at almost 3300 Gy, the signal does not show saturation. Furthermore, since the signal is apparently not bleached, ESR dating of these materials would most likely yield formation ages rather than depositional ages.

5. ESR Spectrometer Design

We have designed and fabricated components of the miniature ESR spectrometer and sample belt as shown in Fig. 6. The frequency-scan ESR spectrometer is achieved by variation of distance (total movement ~ 5 mm) between the two dielectric resonator disks ($\epsilon_R = 29$, 1.0 cm OD x 0.55 cm ID x 0.35 cm thick) using a small DC motor (MicroMo). The sample belt was molded from a silicone rubber material.

C. SIGNIFICANCE OF RESULTS

We have explored the possibility of age dating using polymineral samples and low-temperature OSL, TL characteristics that are essential for Martian in situ age dating. We have fabricated and tested a miniature frequency-scan ESR spectrometer.

D FINANCIAL STATUS

The total funding for this task was \$110,000 all of which has been expended.

E. PERSONNEL

No other personnel were involved in the task.

F. REFERENCES

- [1] D.J. Huntley and M. Lamothe. Ubiquity of anomalous fading in K-feldspars and the measurement and correction for it in optical dating. *Canadian Journal of Earth Sciences* **38**, (2001) 1093-1106.
- [2] M. Lamothe and M. Auclair. A solution to anomalous fading and age shortfalls in optical dating of feldspar minerals. *Earth and Planetary Science Letters* **171**, (1999) 319-323.
- [3] A.S. Murray and A.G. Wintle. Luminescence dating of quartz using an improved single-aliquot regenerative-dose protocol. *Radiation Measurements* **32**, (2000) 57-73.
- [4] R. Visocekas. Monitoring anomalous fading of TL of feldspars by using far-red emission as a gauge. *Radiation Measurements* **32**, (2000) 499-504.
- [5] J. Wallinga, A.S. Murray and A.G. Wintle. The single-aliquot regenerative-dose (SAR) protocol applied to coarse-grain feldspar. *Radiation Measurements* **32**, (2000) 529-533.
- [6] A.G. Wintle. Detailed study of a thermoluminescent mineral exhibiting anomalous fading, 1977.

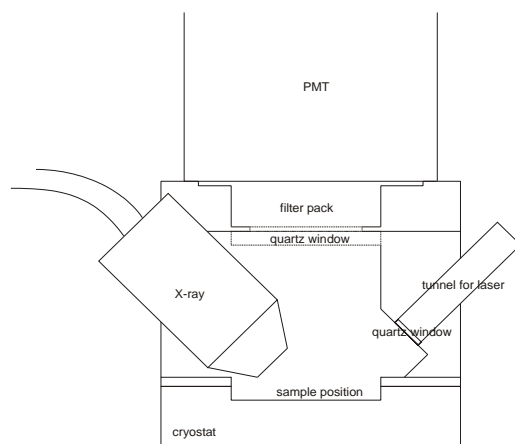


Fig. 1. Diagram of the low-temperature X-ray system.

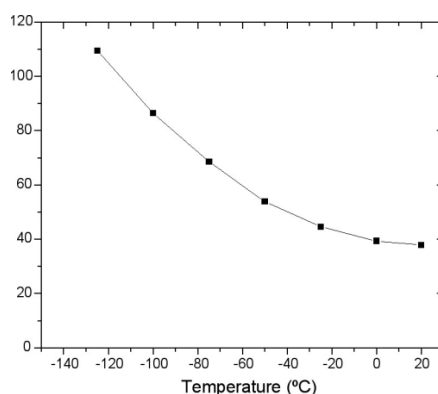


Fig 2. Radioluminescence signal of quartz sample as a function of the sample temperature. The irradiation started at room temperature and the sample was cooled down to -125°C .

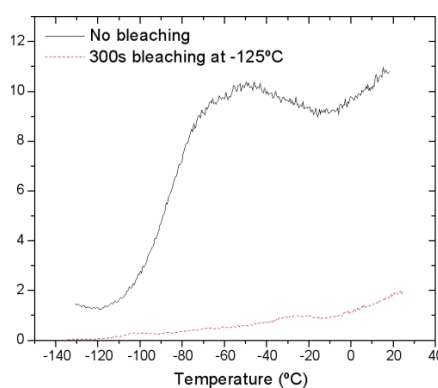


Fig. 3. Effect of bleaching on the low-temperature TL. The sample was irradiated at -125°C with 100 Gy and heated to room temperature at a heating rate of approximately 0.6°C/s (black line). The measurement was repeated introducing a bleaching for 300s at -125°C after irradiation (red line).

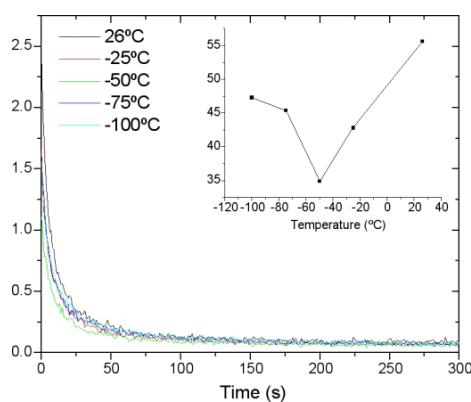


Fig. 4. Effect of measurement temperature on the OSL signal. The sample was irradiated at room temperature (26°C) with 5 Gy and the OSL was subsequently measured at different temperatures.

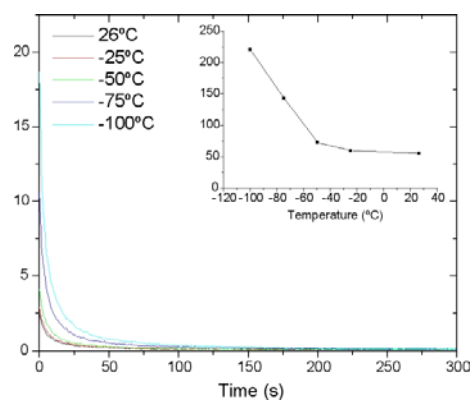


Fig. 5. Effect of irradiation temperature on the OSL measurement. The OSL readout was performed at the same temperature as the irradiation

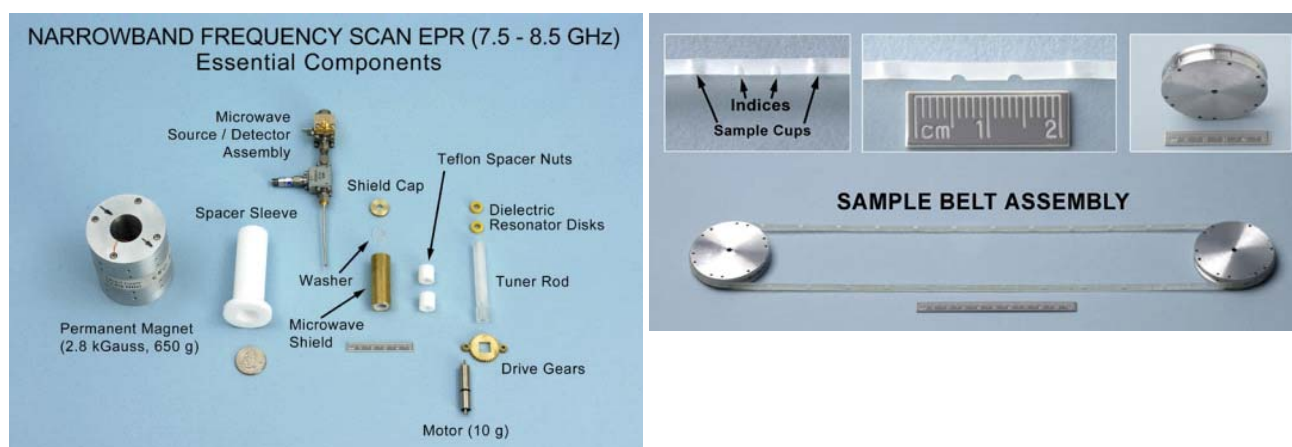


Fig. 6. Essential components of the miniature ESR spectrometer that will be integrated into the Age Dating Instrument. The sample belt was molded from a silicone rubber material.